THE EFFECTS OF TEMPERATURE DEPENDENT VISCOSITY AND VISCOUS DISSIPATION ON MHD CONVECTION FLOW FROM AN ISOTHERMAL HORIZONTAL CIRCULAR CYLINDER IN THE PRESENCE OF STRESS WORK AND HEAT GENERATION

Nabil T.M. Eldabe
Mathematics Department, Faculty of Education,
Ain Shams University, Heliopolis, Cairo, Egypt,
Elsayed M. A. Elbashbeshy,
I. K. Youssef,
Mathematics Department, Faculty of Science,
Ain Shams University, Abbassia, Cairo, Egypt,
Ahmed M. Sedki
Mathematics Department, Faculty of Science,
Ain Shams University, Abbassia, Cairo, Egypt,
Mathematics Department, Faculty of Science,
Jazan University, Jazan, Saudi Arabia

Abstract

Temperature dependent viscosity and Viscous Dissipation effects are considered on hydromagnetic natural convection flow from horizontal circular cylinder immersed in an electrically conducting fluid with viscosity proportional to a linear function of temperature in the presence of stress work and heat generation. The partial differential governing equations are transformed to dimensionless forms. The numerical computations are carried out for several values of physical parameters involved in the transformed equations. The resulting nonlinear system of partial differential equations is solved numerically by Keller box method which is an implicit finite difference technique with Newton's linearization method. The features of the flow and heat transfer characteristics for different values of the governing parameters are analyzed and discussed. To support the accuracy of the numerical results, a comparison is made with known results from the open literature for some particular cases of the present study and the results are found to be in good agreement.

Keywords: Hydromagnetic Convection, Isothermal horizontal circular, Temperature dependent viscosity, Viscous dissipation, Stress work, Heat generation

Nomenclature

a	radius of the circular cylinder	u	fluid velocities in the x-direction
b	the thickness of the cylinder	v	fluid velocities in the y-direction
C_f	local skin-friction coefficient	Greek symbols	
C_p	specific heat at constant pressure	ψ	stream function
Gr	Grashof number	τ_w	shearing stress
g	acceleration due to gravity	ρ	density of the fluid
B_0	strength of the magnetic field	μ	viscosity of the fluid
k	thermal conductivity of the fluid	υ	kinematic viscosity
k_s	thermal conductivity of the solid	γ	viscosity variation parameter
M	magnetic parameter	λ	viscous dissipation parameter
N_T	temperature ratio parameter	ε	pressure stress work parameter
Nu	local Nusselt number	α	conjugate conduction parameter
Pr	Prandtl number	σ_0	electrical conduction coefficient
q	volumetric rate of heat generation	[illegible]	dimensionless temperature function
Q_0	heat generation coefficient	β	coefficient of thermal expansion
Q	heat generation parameter	Subscripts	
T	temperature of the fluid	w	wall conditions
T_∞	temperature of the ambient fluid	∞	ambient temperature
T_w	temperature at the surface	Superscript	
T_b	temperature of cylinder core region	\	differentiation with respect to y

Introduction

Free convection is the principal mode of heat transfer in many applications. In applications in the areas of energy conservation, cooling of electrical and electronics parts, design of solar collectors, free convection may be used to dissipate the energy. Many practical heat transfer applications involved with the conversion of some forms of mechanical, electrical, nuclear or chemical energy to thermal energy are also used this way. The interest in heat transfer and fluid flow problems has grown in the past half century. Since then, a large number of papers have been published viz. Sakiadis (1961), Sparrow (1961), Bliem (1964) and Ackroyd (1974) etc.

A study of natural convection boundary layer flow from an isothermal horizontal cylinder is important from the technical point of view and such types of problems have received much attention by many researchers viz. Merkin (1975), Ingham (1978) and Kuehn *et al*.(1980). Takhar *et al*.(1980) have shown dissipation effects on MHD free convection flow past a semi-infinite vertical plate. Vajravelu and Hadjinolaou (1993) studied the effects of viscous dissipation and internal heat generation on the laminar boundary layer of a viscous fluid flow and heat transfer over a linearly stretching continuous surface. Nazar *et al*.(2000) have considered the problem of natural convection flow on an isothermal horizontal circular cylinder in a micropolar fluid and Molla *et al*.(2006) studied the effect of heat generation on natural convection flow on an isothermal horizontal circular cylinder.

Effects of pressure stress work and viscous dissipation in natural convection flow along a vertical flat plate with heat conduction have been investigated by Alam *et al*. (2006) and Eldabe *et al*.(2012) have investigated the viscous dissipation effect on free convection heat and mass transfer of MHD non-Newtonian fluid flow through a porous medium.

Many authors assumed that the viscosities of the fluid are constant throughout the flow regime. But this physical property may change significantly with temperature. For example, the viscosity of air is 0.6924×10^{-5} kg/ m.s at 100K while it is 3.625 kg/ m.s at 800K temperature, (Cebeci and Bradshaw (1984)). Elbashbeshy *et al*.(2000) investigated the effect of temperature-dependent viscosity on heat transfer over a continuous moving surface. Hossain *et al*.(2000) studied Flow of viscous incompressible fluid with temperature dependent viscosity and thermal conductivity past a permeable wedge with uniform surface heat flux. Molla *et al.*(2012) studied the MHD natural convection flow of a viscous incompressible fluid having viscosity, which is the linear function of temperature, from an isothermal sphere.

Elbashbeshy (2000) studied free convection flow with variable viscosity and thermal diffusivity along a vertical plate in the presence of magnetic field. Azim and Chowdhury (2013) determined the heat transfer process due to hydromagnetic conjugate free convection flow from an isothermal horizontal circular cylinder taking into account stress work and heat generation. Bhuiyan *et al.*(2014) studied joule heating effects on hydromagnetic natural convection flow in presence of viscous dissipation and pressure stress work from a horizontal circular cylinder.

We consider the two-dimensional steady laminar boundary-layer fluid flow and heat transfer process. Temperature dependent viscosity and Viscous Dissipation effects is considered on hydro-magnetic natural convection flow of an electrically conducting fluid from horizontal circular cylinder in the presence of stress work and heat generation .

Mathematical Analysis

MHD laminar free convective flow from an isothermal horizontal circular cylinder of a radius a immersed in a viscous incompressible and conducting fluid with temperature dependent viscosity and viscous dissipation. The effects of the pressure stress work and heat generation is considered. The volumetric rate of heat generation q is considered in the form introduced by Vajravelu K.and Hadjinicolaou A.(1993) as

$$q = \begin{cases} Q_0(T-T_\infty) & for \;\; T \le T_\infty \\ 0 & for \;\; T \ge T_\infty \end{cases}$$

Where Q_0 is the heat generation coefficient, it may be either positive or negative. The source term represents the heat generation when $Q_0 > 0$ and the heat absorption when $Q_0 < 0$. T is the temperature of the fluid within the boundary layer and T_∞ is the ambient temperature of the fluid. A uniform magnetic field having strength B_0 is acting normal to the cylinder surface.

The governing boundary layer equations for the flow characterized with the continuity, momentum and energy equations with the help of Boussinesq approximation are written as:

Fig.1 The physical model and coordinate system

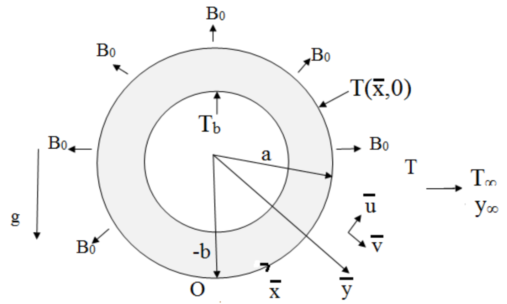

$$\frac{\partial \bar{u}}{\partial \bar{x}} + \frac{\partial \bar{v}}{\partial \bar{y}} = 0 \tag{1}$$

$$\bar{u}\frac{\partial \bar{u}}{\partial \bar{x}} + \bar{v}\frac{\partial \bar{u}}{\partial \bar{y}} = \frac{1}{\rho}\frac{\partial}{\partial \bar{y}}\left(\mu(T)\frac{\partial \bar{u}}{\partial \bar{y}}\right) + g\beta(T-T_\infty)\sin\left(\frac{\bar{x}}{a}\right) - \frac{\sigma_0 B_0^2}{\rho}\bar{u} \tag{2}$$

$$\bar{u}\frac{\partial T}{\partial \bar{x}} + \bar{v}\frac{\partial T}{\partial \bar{y}} = \frac{K}{\rho C_P}\frac{\partial}{\partial \bar{x}}\left(\frac{\partial T}{\partial \bar{y}}\right) + \frac{\mu(\mathrm{T})}{\rho C_P}\left(\frac{\partial \bar{u}}{\partial \bar{y}}\right)^2 + \frac{T\beta}{\rho C_P}\bar{u}\frac{\partial P}{\partial \bar{x}} + \frac{Q_0}{\rho C_P}(T-T_\infty) \tag{3}$$

Where $(\bar{x},\bar{y})$ are the dimensional coordinates along and normal to the tangent of the surface and $(\bar{u},\bar{v})$ are the velocity components parallel to $(\bar{x},\bar{y})$, g is the acceleration due to gravity, $\upsilon_\infty = \mu_\infty/\rho$ is the kinematic viscosity where ρ is the density and μ(T) is the dynamic viscosity of the fluid depending on the fluid temperature T, β is the coefficient of thermal expansion, K is the thermal conductivity of the fluid, σ_0 is the electrical conduction and B_0 is the strength of the magnetic field. The boundary conditions for the velocity components and the temperature are

$$\bar{u} = 0,\;\; \bar{v} = 0 \;\; \text{and} \;\; \mathrm{T}(\bar{x}, 0) = \mathrm{T}_w \;\; on \;\; \bar{y} = 0,\;\; \bar{x} > 0 \tag{4}$$

$$\bar{u} \to 0 \quad and\, T \to T_\infty \;\; as \;\; \bar{y} \to \infty\,,\;\; \bar{x} > 0 \tag{5}$$

The temperature and the heat flux are considered continuous at the interface for the coupled conditions and at the interface we have [12]

$$\frac{\partial T}{\partial \bar{y}} = \frac{\mathrm{k_s}}{\mathrm{k}}\frac{(T - T_b)}{b} \quad on\ \bar{y} = 0,\ \bar{x} > 0$$

where T_∞ is the ambient temperature of the fluid and T_w is the surface temperature of the cylinder. k_s is the thermal conductivity of the solid and k is the thermal conductivity of the fluid. T_b is the temperature of the core region of the cylinder where, $T_b \geq T_\infty$ and b is the normal distance from the inner surface to the outer surface. We will consider the viscosity variation in the form proposed by Charraudeau (1975).

$$\mu(T) = \mu_\infty \left(1 + \gamma^* (T - T_\infty)\right) \tag{6}$$

where μ_∞ is the viscosity of the ambient fluid and γ^* is defined as

$$\gamma^* = \frac{1}{\mu_f}\left(\frac{\partial u}{\partial T}\right)_f$$

Here *f* denotes the film temperature of the fluid. Now we introduce the following non dimensional variables

$$x = \frac{\bar{x}}{a}, \quad y = \frac{\bar{y}}{a} Gr^{1/4}, \quad u = \frac{\rho a}{\mu_\infty} Gr^{-1/2}\,\bar{\mathrm{u}},$$

$$v = \frac{\rho a}{\mu_\infty} Gr^{-1/4} \bar{v}, \quad \theta = \frac{T - T_\infty}{T_b - T_\infty}, \tag{7}$$

$$\mathrm{Gr} = \frac{g\beta(T_b - T_\infty)\,\mathrm{a}^3}{\upsilon_\infty^2}$$

Where θ is the non dimensional temperature, υ_∞ is the reference kinematic viscosity and *Gr* is the Grashof number. Substituting variables in equations (7) into equations (1)-(3), the non dimensional forms of the governing equations are

$$\frac{\partial u}{\partial x} + \frac{\partial v}{\partial y} = 0 \tag{8}$$

$$u\frac{\partial u}{\partial x} + v\frac{\partial u}{\partial y} = (1+\gamma\theta)\frac{\partial^2 u}{\partial y^2} + \gamma\frac{\partial u}{\partial y}\frac{\partial \theta}{\partial y} + \theta \sin x - Mu \tag{9}$$

$$u\frac{\partial \theta}{\partial x} + v\frac{\partial \theta}{\partial y} = \frac{1}{\Pr}\frac{\partial^2 \theta}{\partial y^2} + \lambda(1+\gamma\theta)\left(\frac{\partial u}{\partial y}\right)^2 + Q\theta - \varepsilon\left(N_T + \theta\right)u \tag{10}$$

Where γ is the viscosity variation parameter, *M* is the magnetic parameter, *Pr* is the Prandtl number, λ is the viscous dissipation parameter, *Q* is the heat generation parameter, ε is the pressure stress work parameter and N_T is the temperature ratio parameter, which are defined as

$$\gamma = \gamma^*(T_b - T_\infty) = \frac{1}{\mu_f}\left(\frac{\partial u}{\partial T}\right)_f (T_b - T_\infty), \quad M = \frac{\sigma_0 \beta_0^2 a^2}{\mu_\infty Gr^{1/2}},$$

$$\Pr = \frac{\mu_\infty C_P}{K}, \quad \lambda = \frac{g\beta a}{C_P}, \quad Q = \frac{a^2 Q_0}{\mu_\infty C_P Gr^{1/2}}, \tag{11}$$

$$\varepsilon = \frac{g\beta a}{C_P}, \quad N_T = \frac{T_\infty}{(T_b - T_\infty)}.$$

The boundary conditions can be written in the following non dimensional forms as

$$u = v = 0, \quad \theta - 1 = \alpha \frac{\partial \theta}{\partial y} \quad on\ y = 0, \quad x > 0 \tag{12}$$

$$u \to 0 \quad and \quad \theta \to 0 \ \text{ as } \ y \to \infty, \ x > 0$$

where $\alpha = (bk / ak_s) Gr^{1/4}$ is the conjugate conduction parameter, it depends on the ratios of b/a, k / k_s and Gr. The ratios b/a and k / k_s are less than one where as Gr is large for free convection. Therefore, the value of α may be zero (b=0, for constant cylinder surface temperature) or greater than zero. Throughout this study, we have considered the two cases α=0.0 corresponding constant cylinder surface temperature and α=1 for variable cylinder surface temperature and also we considered the temperature ratio parameter N_t=1.0.

Using boundary layer approximation, the dimensionless variables for the stream function can be introduced as

$$\psi = xf(x, y). \tag{13}$$

where ψ(x,y) is related to the velocity components in the usual way as

$$u = \frac{\partial \psi}{\partial y}, \ v = -\frac{\partial \psi}{\partial x} \tag{14}$$

Substituting in equations (6-9) to obtain the following equations

$$(1+\gamma\theta)\frac{\partial^3 f}{\partial y^3} + f.\frac{\partial^2 f}{\partial y^2} + \gamma \frac{\partial^2 f}{\partial y^2}\frac{\partial \theta}{\partial y} - \left(\frac{\partial f}{\partial y}\right)^2 - M\frac{\partial f}{\partial y} + \theta\frac{\sin x}{x} = x\left(\frac{\partial f}{\partial y}\frac{\partial^2 f}{\partial y \partial x} - \frac{\partial^2 f}{\partial y^2}\frac{\partial f}{\partial x}\right) \tag{15}$$

$$\frac{1}{\Pr}\frac{\partial^2 \theta}{\partial y^2} + f\frac{\partial \theta}{\partial y} + \lambda(1+\gamma\theta)x^2\left(\frac{\partial^2 f}{\partial y^2}\right) + Q\theta - \varepsilon x(N_T + \theta)\frac{\partial f}{\partial y} = x\left(\frac{\partial f}{\partial y}\frac{\partial \theta}{\partial x} - \frac{\partial \theta}{\partial y}\frac{\partial f}{\partial x}\right) \tag{16}$$

The boundary conditions finally become

$$f = \frac{\partial f}{\partial y} = 0 \ \ and \quad \theta - 1 = \alpha \frac{\partial \theta}{\partial y} \ \text{ at } \ \text{y=0}, \ x > 0 \tag{17}$$

$$\frac{\partial f}{\partial y} \to 0 \quad and \quad \theta \to 0 \quad as \quad y \to \infty \ , \ x > 0 \tag{18}$$

The physical quantities of interest in this problem are shearing stress in terms of the skin-friction coefficient and rate of heat transfer which can be written in non dimensional form as follows

$$C_f = \frac{\tau_w}{\rho U_\infty^2}, \text{ and } \quad Nu = \frac{a q_w}{k(\mathrm{T}_w - \mathrm{T}_\infty)} \quad . \tag{19}$$

Where $\tau_w = \mu\left(\frac{\partial \bar{u}}{\partial \bar{y}}\right)_{\bar{y}=0}$ and $q_w = -k\left(\frac{\partial T}{\partial \bar{y}}\right)_{\bar{y}=0}$

Using the non dimensional variables in (19), we get

$$\frac{C_f Gr^{1/4}}{(1+\gamma)} = x\left(\frac{\partial^2}{\partial y^2} f(\mathrm{x},\mathrm{y})\right)_{y=0} \tag{20}$$

$$NuGr^{-1/4} = -\left(\frac{\partial}{\partial y}\theta(\mathrm{x},\mathrm{y})\right)_{y=0} \tag{21}$$

For simplification, we write the notation primes instead of differentiation with respect to y and the heat transfer and the skin friction coefficient in simplified forms as

$$Nux = NuGr^{-1/4} = -\left(\theta'(\mathrm{x},\mathrm{y})\right)_{y=0} \quad \text{and} \quad Cfx = \frac{C_f Gr^{1/4}}{(1+\gamma)} = x\left(f''(\mathrm{x},\mathrm{y})\right)_{y=0}$$

Results and discussion

In this study, we have investigated the boundary layer fluid flow with heat transfer problem of MHD laminar natural convection flow from an isothermal circular cylinder with temperature dependent viscosity in the present of heat generation. The effects of viscous dissipation and pressure stress work are considered. Here, we have considered the viscosity of the fluid proportional to the linear function of temperature that means that if the temperature of the fluid increases, the viscosity also increases. The ordinary partial differential equations (15-16) subjected to the boundary (17-18) are solved numerically using implicit finite difference together with Keller box scheme and the computer programming methods are done in MATLAB. The computations were performed using non uniform grid in the y direction and it was defined by $y_j = sinh((j-1)/100)$, j=1,2,…,605 and Δx=0.01

The velocity profiles, temperature profiles, skin friction and Nusselt numbers are founded for different physical parameters involved in the transformed governing equations. These physical parameters are viscosity variation parameter γ, viscous dissipation parameter λ, Prandlt number Pr, magnetic parameter M, heat generation parameter Q and the pressure stress work ε with constant or variable surface cylinder temperature (i.e. α=0 or α=1). The numerical solutions started at the lower stagnation point x=0 and proceed round the longitude circular cylinder circumference up to the upper stagnation point $x \approx \pi$. For the confirmation of the accuracy of present work, a comparisons of the local Nusselt number Nux and the skin-friction coefficient Cfx obtained in this present work with γ=0.0, λ=0.0, M=0.0, *Pr*=1.0, ε=0.0, *Q*=0.0, *α*=0 and previously reported by Merkin [6] and Molla [18] respectively and a good agreement is founded for the present results as shown in Table 1.

x	$Nux = -\theta'(x,\ 0)$			$Cfx\ = xf''(x,\ 0)$		
	Merkin (1976)	Molla (2006)	Present Work	Merkin (1976)	Molla (2006)	Present Work
0.0	0.421 4	0.4214	0.4213	0.000	0.000	0.000
π/6	0.4161	0.4161	0.4162	0.4151	0.4145	0.4147
π/3	0.4007	0.4005	0.4005	0.7558	0.7539	0.7542
π/2	0.3745	0.3740	0.3741	0.9579	0.9541	0.9543
2π/3	0.3364	0.3355	0.3356	0.9756	0.9696	0.9697
5π/6	0.2825	0.2812	0.2811	0.7822	0.7739	0.7740
π	0.1945	0.1917	0.1916	0.3391	0.3264	0.3264

Table1: Numerical values of *Cfx* and *Nux* for different values of x while *Pr*=1.0, γ=0.0, *λ*=0.0, *M* = 0.0, *Q*=0.0, ε=0.0 and *α*=0.0

We have noted from velocity profiles that the velocity is zero at the boundary wall then the velocity increases up to local maximum value and finally approaches to zero when the boundary layer thickness is the highest, $y=y_\infty$. From isotherm patterns and temperature distributions, we observed that the maximum value for temperature lies on the cylinder surface, *y*=0, and it decreases with the increase of the boundary layer thickness, *y*, then it approaches to zero when the boundary layer thickness is the highest, $y=y_\infty$. Also from isotherm patterns we noted that as *x* increases from the lower stagnation point , *x*=0.0, the hot fluid raises due to the gravity force hence the thickness of the thermal boundary, *y* increases .On other hand we found from streamlines patterns that the non dimensional stream function *ψ* has the minimum value on the cylinder surface, *y*=0, but it increases with increasing of y and finally the maximum value of non dimensional stream function, ψ_{max} ,is determined when the boundary layer thickness is the highest and near the upper stagnation *x*=*π*.

The effect of viscosity variation parameter *γ* on the velocity and temperature distributions against the variable y for different values of the viscosity-variation parameter *γ* (= 0.0, 1.0, 2.0, 3.0, 5.0) at *x*= π/6 are illustrated in figs. (2, 3) while Prandtl number *Pr* =1.0, the viscous dissipation *λ*=0.5, magnetic parameter *M* = 0.1, heat generation *Q*=0.01, pressure stress work ε=0.1and *α*=0.0. It can be noted that with the increasing values of the viscosity variation parameter *γ*, the velocity decreases but for large values of *y* it increases and temperature distribution increases with the increasing values of the viscosity variation parameter γ. We observed that at each value of the viscosity-variation parameter γ, the velocity profile has a maximum value within the boundary layer. The maximum values of the velocity are 0.4073, 0.3371, 0.3008, 0.2763, 0.2434 at y=1.26, 1.71, 2.0, 2.225, 2.56 for γ = 0.0, 1.0, 2.0, 3.0, 5.0 respectively. The maximum velocity decreases by 40.24% as γ increases from 0.0 to 5.0.The numerical values of the skin-friction coefficient Cfx and the local Nusselt number Nux against x for different values of viscosity variation parameter γ while Pr =1.0, λ=0.5, M = 0.1, Q=0.01, ε=0.1and α=0.0 are presented in figs.(4, 5). It is observed that the values of skin-friction coefficient Cfx and the Nusselt number Nux decrease with the increasing values of the viscosity variation parameter. It is due to the increasing of γ, the viscosity of the fluid increases within the boundary layer which retards the fluid motion and as a result, the corresponding skin-friction coefficient Cfx decreases. Due to the temperature of the fluid increases with increasing of the viscosity variation parameter as shown in fig.(3), the corresponding temperature difference between the surface and the fluid enhances and then the rate of heat transfer decreases that means the Nusselt number Nux decreases. The effects of the viscosity variation parameter γ on the streamlines and isotherms distributions are plotted in figs.(6-9) for Pr =1 and λ=0.5, M = 0.1, Q=0.01, ε=0.01 and α=0.0. It can be noted that for each value of γ, the non dimensional value ψ_{max} is near the upper stagnation point (x =π) of the cylinder and when the boundary layer thickness is the highest. We observed that without effect of viscosity-variation (i.e. γ = 0.0), the non dimensional value of ψ_{max} is about 1.40 but it decreases with the increment of γ and ψ_{max} attains about 1.0 for γ = 5.0. In figs.(8, 9), it is shown that the thickness of thermal boundary layer over the surface of the cylinder increases with increment of viscosity variation parameter. That due to the increasing of viscosity variation parameter increases the temperature of the fluid causing increment of the corresponding thermal boundary layer.

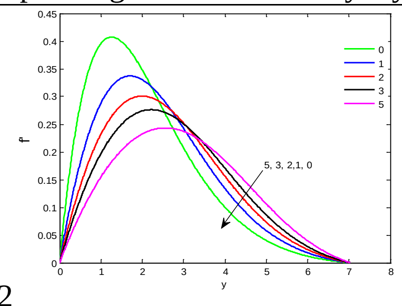

Fig.2

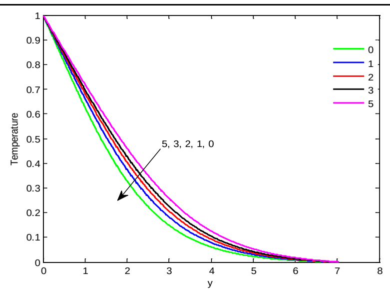

Fig.3

Fig.2: Velocity *for different* γ *with* $\Pr = 1.0, M = 0.1, Q = 0.01, \lambda = 0.5, \varepsilon = 0.1, \alpha = 0.0$

Fig.3: Temperature for different γ *with* $\Pr = 1.0, M = 0.1, Q = 0.01, \lambda = 0.5, \varepsilon = 0.1, \alpha = 0.0$

Fig.4

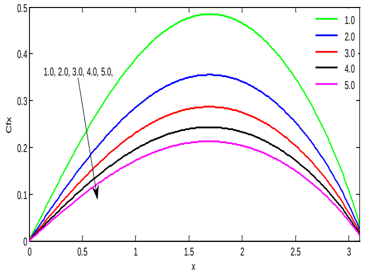

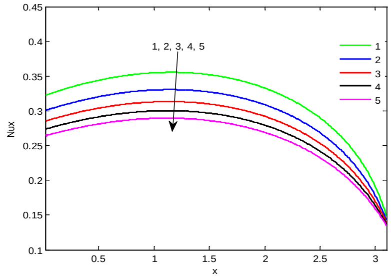

Fig.5

Fig.4: *Cfx for different* γ *with* $\Pr = 1.0, M = 0.1, Q = 0.01, \lambda = 0.5, \varepsilon = 0.1, \alpha = 0.0$
Fig.5: *Nux for different* γ *with* $\Pr = 1.0, M = 0.1, Q = 0.01, \lambda = 0.5, \varepsilon = 0.1, \alpha = 0.0$

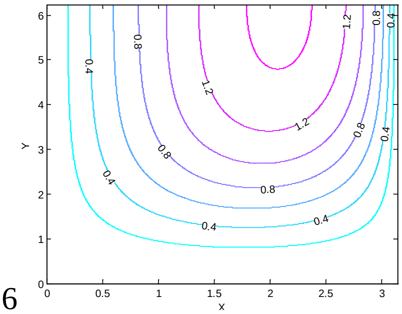

Fig.6

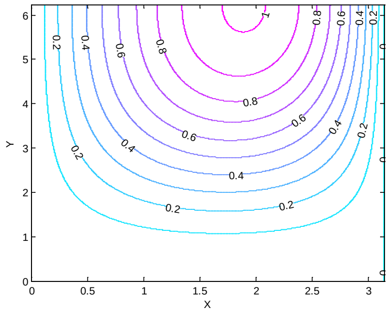

Fig.7

Fig.6: *Streamlines for* $\gamma = 0$, $\Pr = 1$, $M = 0.1$, $Q = 0.01$, $\lambda = 0.5$, $\varepsilon = 0.1, \alpha = 0.0$
Fig.7: *Streamlines for* $\gamma = 5$, $\Pr = 1$, $M = 0.1$, $Q = 0.01$, $\lambda = 0.5$, $\varepsilon = 0.1, \alpha = 0.0$

Fig.8

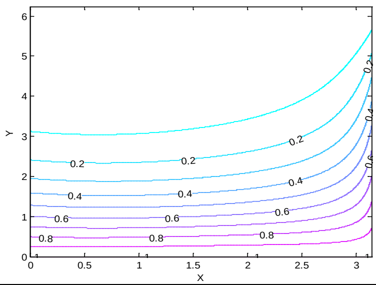

Fig.9

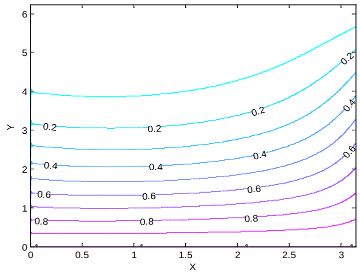

Fig.8: *Streamlines for* $\gamma = 0$, $\Pr = 1$, $M = 0.1$, $Q = 0.01$, $\lambda = 0.5$, $\varepsilon = 0.1, \alpha = 0.0$
Fig.9: *Isotherms for* $\gamma = 5$, $\Pr = 1$, $M = 0.1$, $Q = 0.01$, $\lambda = 0.5$, $\varepsilon = 0.1, \alpha = 0.0$

The effects of viscous dissipation parameter variation λ on the velocity and temperature profiles while Pr = 1.0, M = 0.1, γ = 0.5, Q = 0.01, α=1.0 and $\mathcal{E}$=0.1 at x= π/6 are presented in figs.(10,11). It can be observed that the velocity and temperature distributions increase with the increasing values of the viscous dissipation parameter λ. The maximum values of the velocity are 0.2833, 0.2903, 0.306 and 0.3245 for λ =0.0, 1.0, 3.0 and 5.0 respectively at position y=1.485. Counting these peak values of the velocity, we have calculated that the velocity rises by 14.54 % as λ increases from 0.0 to 5.0. The skin-friction coefficient Cfx and the local Nusselt number Nux distributions against x for different values of viscous dissipation parameter λ while γ=0.5, Pr =1.0, λ=0.1, M = 0.1, Q=0.01, $\mathcal{E}$=0.1 and α=1.0 are presented in figs.(12, 13). It is observed that the increasing of the viscous dissipation parameter λ increases the skin friction and decreases the rate of heat transfer.

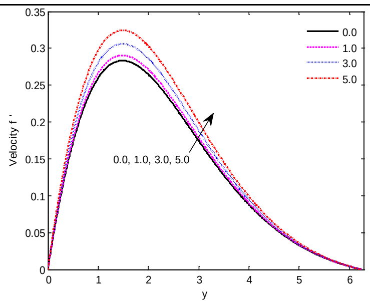

Fig.10

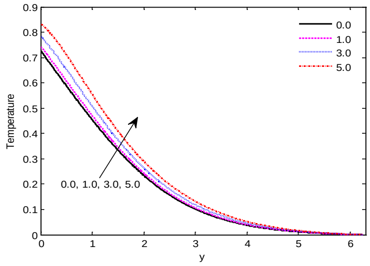

Fig.11

$Fig.10$: *Velocity for different* λ *with* $\gamma = 0.5,\ \Pr = 1.0,\ M = 0.1,\ Q = 0.01,\ \alpha = 1.0, \varepsilon = 0.1$

$Fig.11$: *Temperature for different* λ *with* $\gamma = 0.5,\ \Pr = 1.0,\ M = 0.1,\ Q = 0.01,\ \alpha = 1.0, \varepsilon = 0.1$

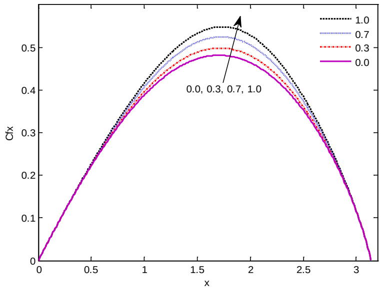

Fig.12

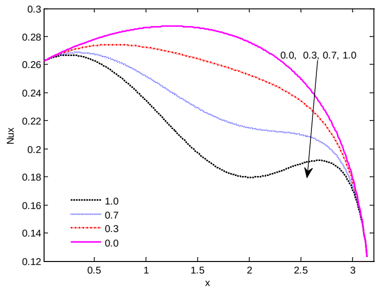

Fig.13

$Fig.12$: *cfx for different* λ *with* $\gamma = 0.5,\ \Pr = 1.0,\ M = 0.1,\ Q = 0.01,\ \alpha = 1.0, \varepsilon = 0.1$

$Fig.13$: *Nux for different* λ *with* $\gamma = 0.5,\ \Pr = 1.0,\ M = 0.1,\ Q = 0.01,\ \alpha = 1.0, \varepsilon = 0.1$

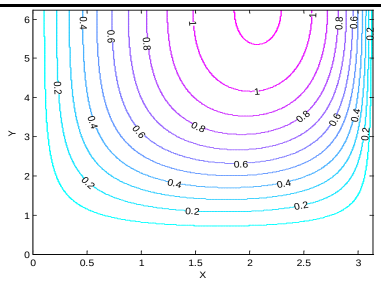

Fig.14

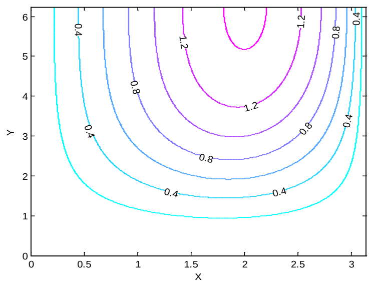

Fig.15

Fig.14: *Streamlines for* $\lambda = 0.0$ *with* $\gamma = 0.5,\ \Pr = 1.0,\ M = 0.1,\ Q = 0.01,\ \alpha = 1.0, \varepsilon = 0.1$

Fig.15: *Streamlines for* $\lambda = 1.5$ *with* $\gamma = 0.5,\ \Pr = 1.0,\ M = 0.1,\ Q = 0.01,\ \alpha = 1.0, \varepsilon = 0.1$

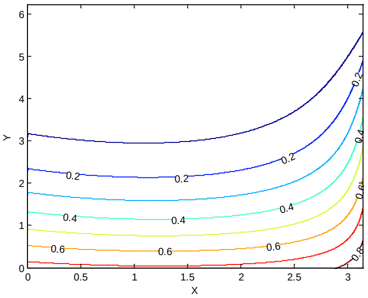

Fig.16

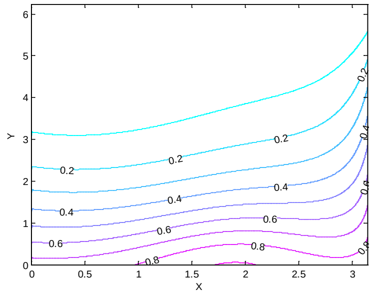

Fig.17

Fig.16: *Temperature for* $\lambda = 0.0$ *with* $\gamma = 0.5,\ \Pr = 1.0,\ M = 0.1,\ Q = 0.01,\ \alpha = 1.0, \varepsilon = 0.1$

Fig.17: *Temperature for* $\lambda = 1.5$ *with* $\gamma = 0.5,\ \Pr = 1.0,\ M = 0.1,\ Q = 0.01,\ \alpha = 1.0, \varepsilon = 0.1$

It is seen from figs.(14,15) that without effect of viscous dissipation parameter (i.e. λ = 0.0) the non dimensional value of ψ_{max} is about 1.10 and it increases with the increment of λ until ψ_{max} attains about 1.40 for λ= 5.0 (see fig. 15). This phenomenon coincides with the early discussion, the fluid velocity increases as λ increases and the thickness of the velocity boundary layer also increases.

The isotherm patterns for corresponding values of λ are illustrated in figs.(16,17). From these two frames it can be noted that for λ=1.5, the maximum value of temperature which lies on the surface of the cylinder is about 0.90658 at *x*=1.91 but without effect of viscous dissipation parameter (i.e. λ = 0.0), it is about 0.88266 at the upper stagnation point x=π. This phenomenon can be understood from the fact that the increasing values of viscous dissipation parameter increase the temperature and decrease the rate of heat transfer as shown in figs.(11,13).

The effects of magnetic parameter *M* on the velocity and temperature distributions are shown in figs.(18,19) against *y* with Prandlt number *Pr*, viscous variation parameter γ, heat generation parameter *Q* and viscous dissipation parameter λ. Here it is found that the velocity decreases and the temperature increases with the increasing of the magnetic parameter. We observed from fig.18 that for M=0.0, 0.2, 0.5, 0.8 and 1.0, the maximum values of the velocity are 0.2859, 0.2602, 0.2299, 0.2065 and 0.1936 at x=1.66, 1.635, 1.595, 1.56 and 1.54 respectively. We have found that the maximum velocity decreases by 32.28% as *M* increases from 0.0 to 1.0.

The variation of the local skin friction coefficient *Cfx* and the local rate of heat transfer *Nux* for the values of magnetic parameter *M* (= 0.1, 0.3, 0.5, 0.7) with γ =1.0, Pr = 1.0, λ=1.0, Q=0.01, α=1.0 and ε=0.1 are shown in figs.(20, 21), respectively. It is clear that the skin-friction and heat transfer coefficients decrease with the increasing values of magnetic parameter. This phenomenon comes from the fact that the increment of magnetic parameter M increases the effect of Lorentz force which opposes the fluid flow and hence the fluid velocity and temperature gradient decrease. The effect of the magnetic parameter M on the streamlines and isotherms are demonstrated in figs. (22-25) which are plotted for Pr =1, γ=1.0, λ=1.0, Q=0.01, ε=0.1 and α=1.0 From figs.(22,23), it is seen that without effect of magnetic parameter M (i.e. M = 0.0), the non dimensional value of ψ_{max} is about 1.2 and ψ_{max} decreases with the increment of M and it attains about 0.7 for M= 1.0 (see fig. 23). The isotherm patterns for corresponding values of M are shown in figs.(24,25). We can see that the thermal boundary layer over the surface of the cylinder increases with the increasing of the magnetic parameter M. Also from these figures, it can be noted that for the selected values of M, the maximum values of temperature lie at the upper stagnation point of the cylinder, x=π, and it is about 0.88298 for M=1.0 but without effect of viscous dissipation parameter (i.e. M = 0.0), the maximum value of temperature is about 0.88306

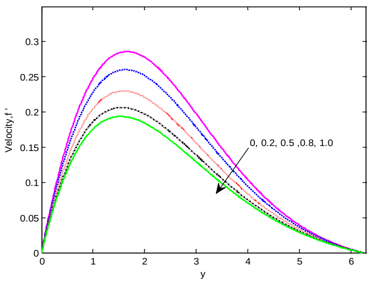

Fig.18

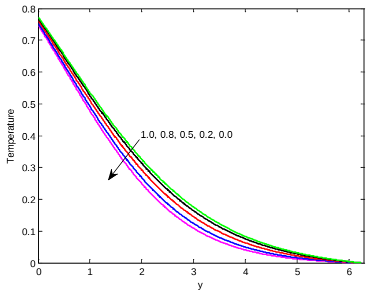

Fig.19

Fig.18: Velocity for different M with $\gamma = 1.0, \Pr = 1.0, Q = 0.01, \lambda = 1.0, \varepsilon = 0.1, \alpha = 1$

Fig.19: Temperature *for* different M with $\gamma = 1.0,\ \Pr = 1.0,\ Q = 0.01,\ \lambda = 1.0,\ \varepsilon = 0.1,\ \alpha = 1$

Fig.20

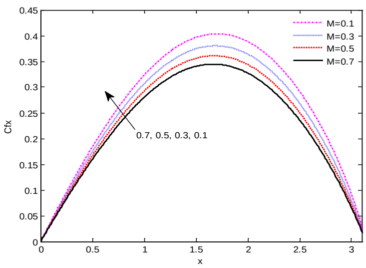

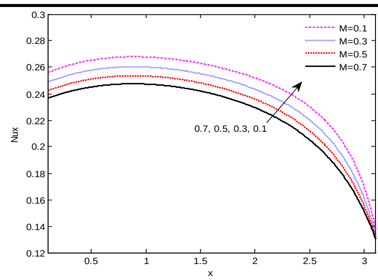

Fig.21

Fig.20: The Heat transfer *for* different M with $\gamma = 1.0, \Pr = 1.0, Q = 0.01, \lambda = 1.0, \varepsilon = 0.1, \alpha = 1$

Fig.21: The Skin friction *for* different M with $\gamma = 1.0, \Pr = 1.0, Q = 0.01, \lambda = 1.0, \varepsilon = 0.1, \alpha = 1$

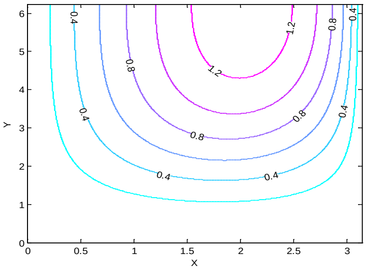

Fig.22

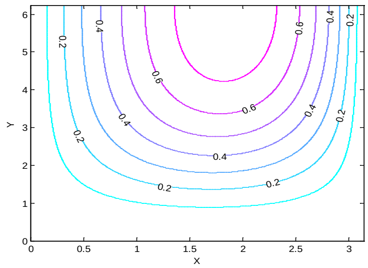

Fig.23

Fig.22: Streamlines *for* M=0.0 with $\gamma = 1.0, \Pr = 1.0, Q = 0.01, \lambda = 1.0, \varepsilon = 0.1, \alpha = 1$

Fig.23: Streamlines *for* M=1.0 with $\gamma = 1.0, \Pr = 1.0, Q = 0.01, \lambda = 1.0, \varepsilon = 0.1, \alpha = 1$

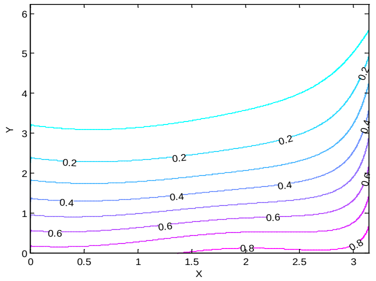

Fig.24

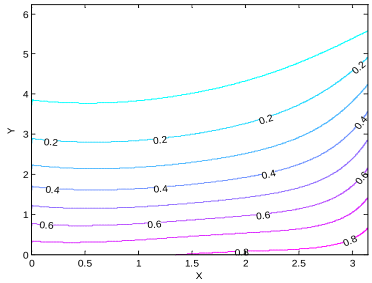

Fig.25

Fig.24: Isotherms *for* M=0.0 with $\gamma = 1.0, \Pr = 1.0, Q = 0.01, \lambda = 1.0, \varepsilon = 0.1, \alpha = 1$

Fig.25: Isotherms *for* M=1.0 with $\gamma = 1.0, \Pr = 1.0, Q = 0.01, \lambda = 1.0, \varepsilon = 0.1, \alpha = 1$

The effects of the Prandtl number *Pr* with γ=1.0, λ=0.5, *M* = 0.1, *Q*=0.01, ε = 0.1 and α =1.0 on the velocity profiles and the temperature profiles are indicated in figs.(26, 27). It is observed that the increasing values of Prandtl number *Pr* leads to the decrease in the velocity profiles. For the values of Prandtl number *Pr* = 0.73, 1.0, 1.44, 1.63 and 2.0, the maximum values of the velocity are 0.297, 0.2695, 0.2379, 0.2273 and 0.2104 which occur at *y* = 1.71, *y* = 1.645, *y* = 1.56, 1.535 and *y* = 1.49 respectively. Here it is found that the velocity decreases by 29.16% as *Pr* increases from 0.73 to 2.0. From fig.(27), we noted that the temperature profiles decreases with the increasing values of Prandtl number *Pr*. That is due to the Prandtl number is the ratio of viscous force and thermal force. Thus the increasing of *Pr* increases viscosity and decreases the thermal action of the fluid and hence decreases the velocity and the temperature of the fluid. The effect of the Prandtl number *Pr* on skin friction and the rate of heat transfer are shown in figs. (28, 29) with γ = 1.0, λ=0.5, *M* =0.10, *Q* = 0.01, α=1.0 and ε=0.1. We observed that the increment of *Pr* leads to the decrease of the skin friction coefficient *Cfx* and the increase of heat transfer rate *Nux*. It is due to the decreasing of the fluid velocity leads to the decrease of skin friction and the decreasing of temperature within the boundary layer increases temperature difference between core region and outer surface of the cylinder which leads to increasing rate of heat transfer from the core region to the boundary layer as noted in figs.(28,29) respectively. The effect of the Prandtl number *Pr* on the development of streamlines and isotherms are shown in figs.(30-33) which are plotted for, γ=1.0, λ=0.5, *M*=0.1, ε=0.1, *Q*=0.01 and α=1.0. It is seen from these figures that the value of ψ_{max} within the computational domain is about 1.2 with Prandtl number *Pr*=0.73 and ψ_{max} decreases with the increment of *Pr* and it attains about 0.8 for *Pr*= 2.0 (see Fig.31). The isotherm patterns for corresponding values of *Pr* are shown in figures (32, 33). It can noted that the thermal boundary layer over the surface of the cylinder for *Pr*=0.73 is greater than for *Pr*=2.0 and hence we can said that the thickness of the thermal boundary layer decreases as *Pr* increases.

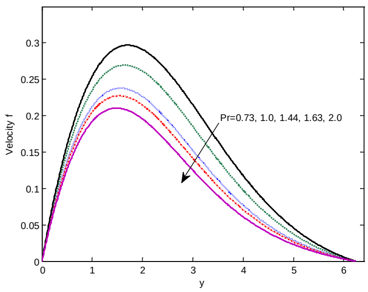

Fig.26

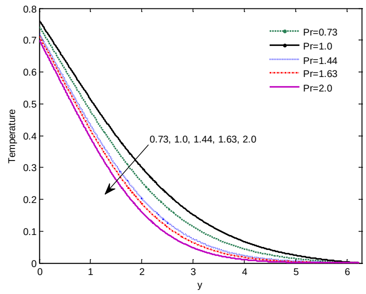

Fig.27

Fig.26:Velocity *for* different Pr with $\gamma = 1.0, \lambda = 0.5, M = 0.1, Q = 0.01, \varepsilon = 0.1, \alpha = 1$

Fig.27: Temperature *for* different Pr with $\gamma = 1.0, \lambda = 0.5, M = 0.1, Q = 0.01, \varepsilon = 0.1, \alpha = 1$

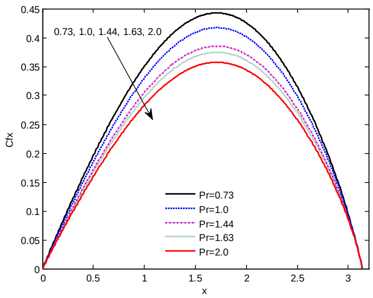

Fig.28

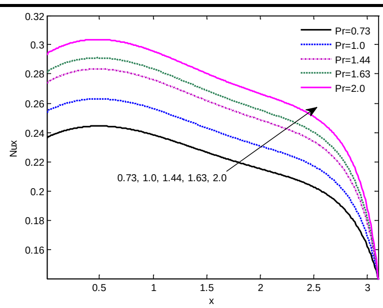

Fig.29

Fig.28: Heat transfer *for* different values of Pr with $\gamma = 1.0, \lambda = 0.5, M = 0.1, Q = 0.01, \varepsilon = 0.1, \alpha = 1$

Fig.29 : Skin Friction *for* different values of Pr with $\gamma = 1.0, \lambda = 0.5, M = 0.1, Q = 0.01, \varepsilon = 0.1, \alpha = 1$

Fig.30

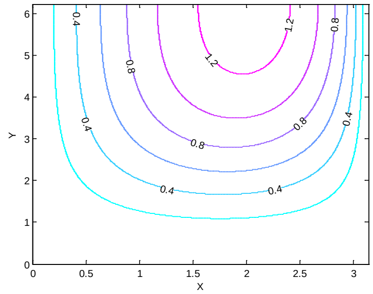

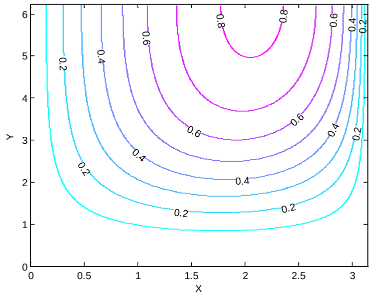

Fig.31

Fig.30: Streamlines *for* Pr=0.73 with $\gamma = 1.0, \lambda = 0.5, \mathrm{M} = 0.1, Q = 0.01, \varepsilon = 0.1, \alpha = 1$

Fig.31: Streamlines *for* Pr=2.0 with $\gamma = 1.0, \lambda = 0.5, \mathrm{M} = 0.1, Q = 0.01, \varepsilon = 0.1, \alpha = 1$

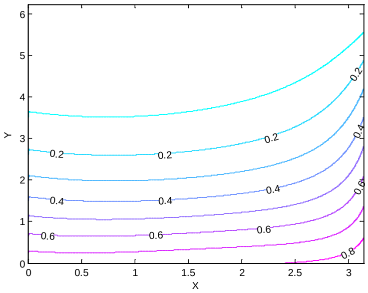

Fig.32

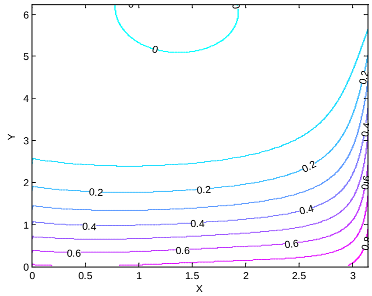

Fig.33

Fig32: Isotherms *for* Pr=0.73 with $\gamma = 1.0, \lambda = 0.5, \mathrm{M} = 0.1, Q = 0.01, \varepsilon = 0.1, \alpha = 1$

Fig.33: Streamlines *for* Pr=2.0 with $\gamma = 1.0, \lambda = 0.5, \mathrm{M} = 0.1, Q = 0.01, \varepsilon = 0.1, \alpha = 1$

The effects of pressure stress work ε on the velocity and temperature distributions are displayed in figs. (34, 35) for different values of the pressure stress work ε with Prandlt number Pr = 1.0, magnetic parameter M=0.1, viscous variation parameter γ = 1.0, viscous dissipation parameter λ=0.5, heat generation parameter Q=0.01and α=1.0. We observed in these figures that the velocity and temperature profiles decrease with the increasing of pressure stress work. The stress work parameter contains gravitational force g which works against the buoyancy force. As a result the motion of the fluid decreases with increasing values of ε and hence the velocity and temperature decrease with the increasing of pressure stress work. The upper limit of the velocity are 0.2853, 0.2688, 0.2522 and 0.2123 for ε=0.01, 0.1, 02 and 0.5 at x=1.67, 1.645, 1.61and 1.515 respectively.We found that the velocity decreases by 25.57 % as ε count in from 0.01 to 0.5. The effect of the pressure stress work on skin friction and the rate of heat transfer are shown in figs. (36, 37) with Pr = 1.0, M =0.1, γ = 1.0, λ=0.5, Q=0.01 α=1.0 and ε=0.1. We observed that the skin friction coefficient decreases with the increasing of stress work parameter and we found that the skin friction coefficient decreases by 35.45% for ε count in from 0.01 to 0.5. From fig. 37, we observed that the heat transfer rate increases with increasing stress work parameter ε along x direction. That is due to the decreased temperature for increasing stress work parameter within the boundary layer reduced the temperature difference between the boundary layer region and the core region which increases heat transfer rate and local Nusselt number increased. The effect of the pressure stress work parameter on the streamlines and isotherms are shown in figures (38-41) which are plotted for Pr =1, γ=1.0, λ=0.5, M=0.1, Q=0.01 and α=1.0. From figs.(38, 39), it can be noted that the value of ψ_{max} is about 1.4 with pressure stress work $\mathcal{E}$=0.01 and ψ_{max} decreases with the increment of $\mathcal{E}$ and it attains about 0.55 for $\mathcal{E}$= 0.5 hence it can be said that the streamlines decrease with the increasing values of the pressure stress work. The isotherm patterns for corresponding values of $\mathcal{E}$ are shown in figs.(40, 41). From these figures, it can be noted that the thickness of the thermal boundary layer increases as x increases from the lower stagnation point ($x \approx 0.0$). This phenomenon can be understood from the fact that the hot fluid raises due to the gravity force g in pressure stress work ε hence the thickness of the thermal boundary layer increases.

Fig.34

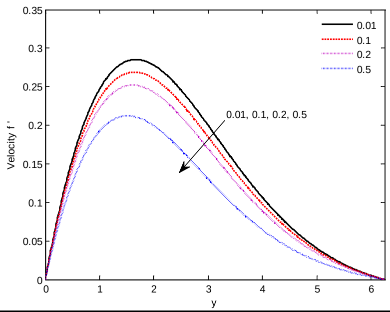

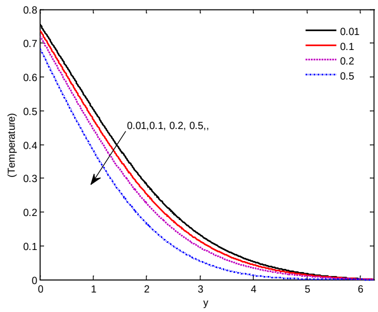

Fig.35

Fig34: Velocity *for* different values of ε with Pr=1.0 $\gamma = 1.0, \lambda = 0.5, M = 0.1, Q = 0.01, \alpha = 1$

Fig.35: Temperature *for* different values of ε with Pr=1.0 $\gamma = 1.0, \lambda = 0.5, M = 0.1, Q = 0.01, \alpha = 1$

Fig.36

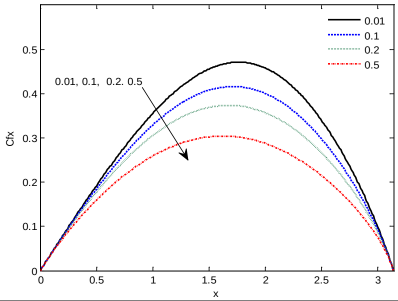

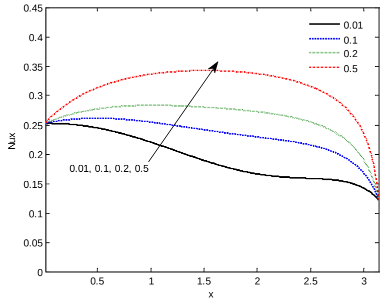

Fig.37

Fig.36: Cfx *for* different values of ε with Pr=1.0 $\gamma=1.0, \lambda=0.5, M=0.1, Q=0.01, \alpha=1$

Fig.37: Nux *for* different values of ε with Pr=1.0 $\gamma=1.0, \lambda=0.5, M=0.1, Q=0.01, \alpha=1$

Fig.38

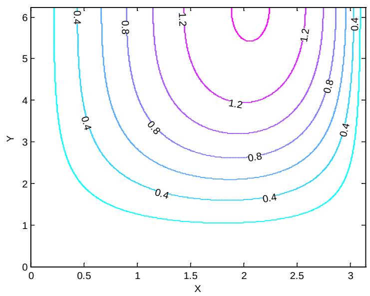

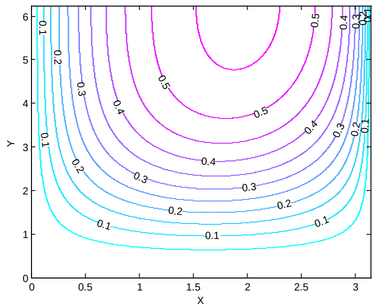

Fig.39

Fig.38: *Streamlines* for $\varepsilon=0.01$ with Pr=1.0 $\gamma=1.0, \lambda=0.5, M=0.1, Q=0.01, \alpha=1$

Fig.39: *Streamlines* for $\varepsilon=0.5$ with Pr=1.0 $\gamma=1.0, \lambda=0.5, M=0.1, Q=0.01, \alpha=1$

Fig.40

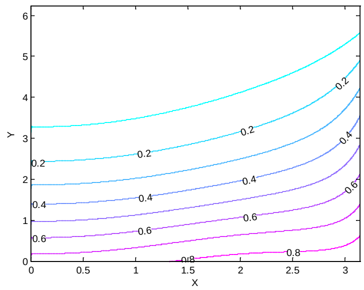

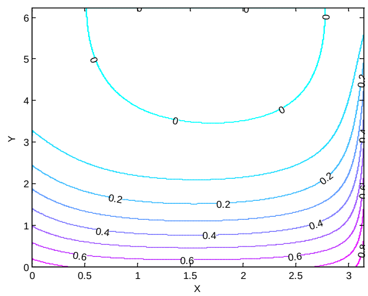

Fig.41

Fig.40: *Temperature* for $\varepsilon=0.01$ with Pr=1.0 $\gamma=1.0, \lambda=0.5, M=0.1, Q=0.01, \alpha=1$

Fig.41: *Temperature* for $\varepsilon=0.5$ with Pr=1.0 $\gamma=1.0, \lambda=0.5, M=0.1, Q=0.01, \alpha=1$

The effects of heat generation Q on the velocity and temperature distributions are displayed in figs.(42, 43) with Prandtl number Pr = 1.0, viscous variation parameter γ = 1.0, viscous dissipation parameter λ = 0.5, magnetic parameter M = 0.1, pressure stress work $\mathcal{E}$=0.1 and conduction parameter α=1.0. It is observed that the velocity and temperature profile increase with the increasing of heat generation parameter. The maximum values of the velocity are 0.2688, 0.2820, 0.2928 and 0.308 for Q =0.01, 0.05, 0.08 and 0.12, respectively, which come at x=1.665. We found that the velocity increases by 14.583% as Q count in from 0.01 to 0.12.

The effect of heat generation parameter Q on skin friction and the rate of heat transfer are shown in Figures (44, 45) with Pr = 1.0, M =0.10, γ = 1.0, λ = 0.10, α=1.0 and $\mathcal{E}$=0.1. We observed that for increment of Q, the skin friction coefficient increases; on the other hand the heat transfer rate decreases along x direction and we found that the maximum values of the skin friction coefficient increases by 14.83% but local Nusselt number decreases by 26.87%, for varying of Q from 0.01 to 0.12. From fig.44 it can be seen that the skin friction coefficient values are negative near the upper stagnation point, $x=\pi$, of the cylinder surface for large values of heat generation parameter Q.

The effect of the heat generation parameter Q on the development of streamlines and isotherms are shown in figures (46-49) which are plotted for Pr =1, γ=1.0, λ=0.5, M=0.1, $\mathcal{E}$=0.1 and α=1.0. It is seen from figs.(46, 47) that the value of ψ_{max} is about 1.1 near the upper stagnation point (x =π) of the cylinder with the heat generation parameter Q=0.01and ψ_{max} increases with the increment of Q and it attains about 1.4 for Q= 0.12.

Fig.42

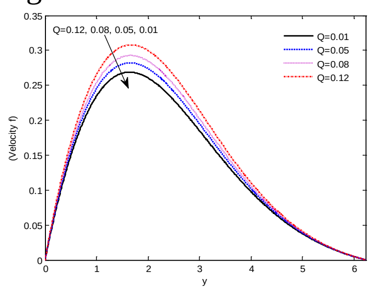

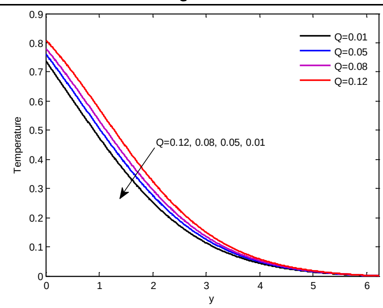

Fig.43

Fig.42: Velocity *for* different values of Q with Pr=1.0 $\gamma=1.0, \lambda=0.5, M=0.1, \varepsilon=0.1, \alpha=1$
Fig.43: Velocity *for* different values of Q with Pr=1.0 $\gamma=1.0, \lambda=0.5, M=0.1, \varepsilon=0.1, \alpha=1$

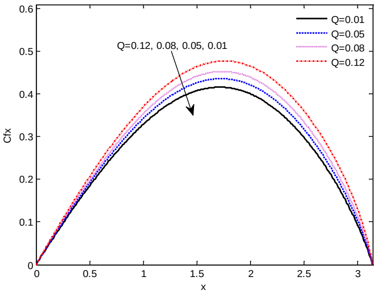

Fig.44

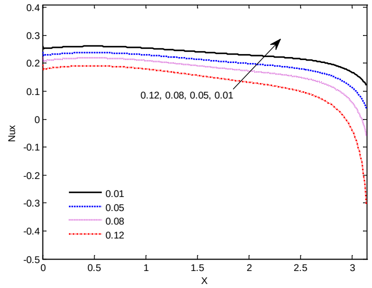

Fig.45

Fig.44: Cfx *for* different values of Q with Pr=1.0 , $\gamma = 1.0, \lambda = 0.5, M = 0.1, \varepsilon = 0.1, \alpha = 1$

Fig.45: Nux *for* different values of Q with Pr=1.0 , $\gamma = 1.0, \lambda = 0.5, M = 0.1, \varepsilon = 0.1, \alpha = 1$

Fig.46

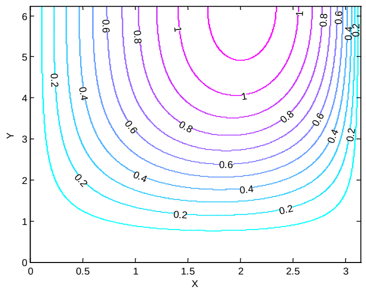

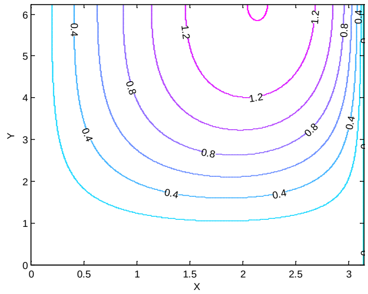

Fig.47

Fig.46: Streamlines *for* $Q = 0.01$ with Pr=1.0 $\gamma = 1.0, \lambda = 0.5, M = 0.1, \varepsilon = 0.1, \alpha = 1$

Fig 47: Streamlines *for* $Q = 0.12$ with Pr=1.0 $\gamma = 1.0, \lambda = 0.5, M = 0.1, \varepsilon = 0.1, \alpha = 1$

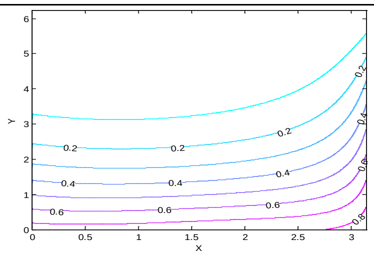

Fig.48

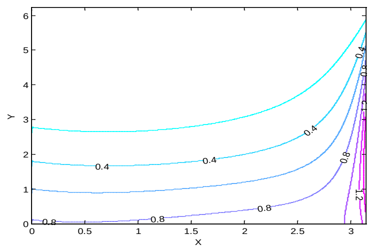

Fig.49

Fig.48: Isotherms *for* $Q = 0.01$ with Pr=1.0 $\gamma = 1.0, \lambda = 0.5, M = 0.1, \varepsilon = 0.1, \alpha = 1$

Fig 49: Isotherms *for* $Q = 0.12$ with Pr=1.0 $\gamma = 1.0, \lambda = 0.5, M = 0.1, \varepsilon = 0.1, \alpha = 1$

The isotherm patterns for corresponding values of Q are shown in figs.(48,49). We can see that the thermal boundary layer over the surface of the cylinder for Q=0.01 is greater than for Q=0.12 and we noted in fig.48 that for Q=0.01, the fluid temperature increases sharply at the upper stagnation point, x=π.

Conclusion

The effect of temperature-dependent viscosity and viscous dissipation on the MHD natural convection boundary layer flow from an isothermal horizontal circular cylinder in the presence of pressure stress work and heat generation has been investigated. Numerical solutions of the equations governing the flow are obtained by using the very efficient implicit finite difference method together with Keller box scheme. From the present investigation the following conclusions may be drawn:

1. The local skin-friction coefficient cfx grows as a result of the increment of the velocity profile, on other hand the increment of the temperature distribution leads to the decrease of the local Nusselt number Nux.
2. The local skin-friction coefficient cfx decreases with the increment of the viscosity variation parameter γ, the magnetic parameter M, the pressure stress work parameter ε and the Prandtl parameter Pr but cfx increases with the increment of viscous variation parameter λ and heat generation parameter Q.
3. The local Nusselt number Nux decreases with the increment of the viscosity variation parameter γ, the magnetic parameter M, the viscous dissipation parameter λ and heat generation parameter Q but Nux decreases with the increment of the pressure stress work ε and the Prandtl parameter Pr.
4. The maximum value of non dimensional stream function ψmax which lies near the upper stagnation $x=\pi$ and when the boundary layer thickness is the highest, increases with the increment of viscous dissipation parameter λ and heat generation parameter Q but ψmax decreases with the increment of viscosity dissipation parameter λ, the pressure stress work, Prandtl number parameter Pr and the magnetic parameter M.
5. The thermal boundary layer extends with the increasing values of the viscosity variation parameter γ and the magnetic parameter M but it decreases with increasing values of Prandtl number Pr and heat generation parameter Q.
6. The results have shown that, in order to get the accurate behavior of the flow, the variation of fluid properties are necessary to take into account and the assumption of constant fluid properties may leads to errors in the evaluation of the surface shearing stress and the rate of heat transfer.

References:

Sakiadis B. C., (1961), Boundary layer behavior on continuous solid surfaces. III. The boundary layer on a continuous cylindrical surface. A.I.Ch.E.J. 7, 467-472.

Sparrow E. M. and Cess R. D., (1961), Effect of magnetic field on free convection heat transfer, Int. J of Heat and Mass Transfer 3, 267-274.

Carl John Bliem Jr , (1964), Free convection heat transfer from the outside of a vertical Isothermal circular cylinder, School of Mechanical Engineering, Georgia Institute of Technology.

Ackroyd J. A. D., (1974), Stress work effects in laminar flat-plate natural convection, J. of Fluid Mech. 62, 677–695.

Charraudeau J., (1975), Influence de gradients de properties physiques en convection force application au cas du tube, Int. J. Heat Mass Trans. 18, 87-95.

Merkin J.H. , (1976), Free convection boundary layer on an isothermal horizontal circular cylinders, ASME/AIChE, Heat Transfer Conference, St. Louis Mo., August 911.

Ingham D.B., (1978), Free convection boundary layer on an isothermal horizontal cylinder, Z. Angew. Math. Phys. 29, 871-883.

Keller H.B., (1978), Numerical methods in boundary layer theory, Annual Rev. Fluid Mech., 10, 417-433.

Kuehn T.H. and Goldstein R.J., (1980), Numerical solution to the Navier-Stokes equations for laminar natural convection about a horizontal isothermal circular cylinder, Int. J. heat Mass Transfer 23, 971-979.

Takhar, H.S. and V.M. Soundalgekar, (1980), Dissipation effects on MHD free convection flow past a semi-infinite vertical plate, Applied Science Research, 36, 163-171.

Cebeci T., Bradshaw P.,(1984), Physical and Computational Aspects of Convective heat Transfer, Springer, New York.

Merkin, J. H. and I. Pop,(1988), A note on the free convection boundary layer on a horizontal circular cylinder with constant heat flux, Wärmend Stoffübertragung 22, 79-81.

Vajravelu K., Hadjinicolaou A.,(1993), Heat transfer in a viscous fluid over a stretching sheet with viscous dissipation and internal heat generation, Int. Comm. Heat Mass Transfer 20, 417–430.

Elbashbeshy E. M. A., Bazid M. A. A.,(2000), The effect of temperature-dependent viscosity on heat transfer over a continuous moving surface, J. Phys. D: Appl. Phys. 33, 2716. doi:10.1088/0022-3727/33/21/309

Hossain M.A., Munir M.S., Rees D.A.S.,(2000), Flow of viscous incompressible fluid with temperature dependent viscosity and thermal conductivity past a permeable wedge with uniform surface heat flux, Int. J. Therm. Sci. 39, 635-644

Elbashbeshy, E. M. A.,(2000), Free Convection Flow with Variable Viscosity and Thermal Diffusivity along a Vertical Plate in the Presence of Magnetic Field, Int. J. Eng. Science, 38(2), 207-213, doi:10.1016/S0020-7225(99)00021-x

Nazar R., Amin N., Pop I.,(2000), Free convection boundary layer on an isothermal horizontal circular cylinder in a micropolar fluid, Heat Transfer, Proceeding of the Twelfth International Conference.

Molla M.M, Hossain M.A., Paul M. C.,(2006), Natural convection flow from an isothermal horizontal circular cylinder in presence of heat generation, Int. J. Eng. Sci. 44, 949-958.

Alam, M., A. Alim and M.K. Chowdhury,(2006), Effect of pressure stress work and viscous dissipation flow along a vertical flat plate with heat conduction, journal of naval architecture and marine engineering 3(2) 69- 76.

Nabil T. M. Eldabe, Sallam N. Sallam, Mohamed Y. Abou-zeid, (2012), Numerical study of viscous dissipation effect on free convection heat and mass transfer of MHD non Newtonian fluid flow through a porous medium, Journal of the Egyptian Mathematical Society.

Molla, M. M., Saha C. and Hossain M.A., (2012), The effect of temperature dependent viscosity on MHD natural convection flow from an isothermal sphere, Journal of Applied Fluid Mechanics 5(2) 25-31.

Azim N. H. M. A. and Chowdhury M. K., (2013), Hydromagnetic conjugate free convection flow from an Isothermal Horizontal Circular cylinder With Stress Work and Heat Generation, international journal of energy & technology 5 (17) 1–9.

Bhuiyan A. S., Azim N. H. M. A. and Chowdhury M. K., (2014) , Joule Heating Effects on MHD Natural Convection Flows in Presence of Pressure Stress Work and Viscous Dissipation from a Horizontal Circular Cylinder, Journal of Applied Fluid Mechanics 7(1) 7-13

Nabil T. M. Eldabe, Ahmed M. Sedki, I. K. Youssef,(2014), Numerical solutions for boundary layer fluid flow with mass transfer over a moving permeable flat plate embedded in porous medium with variable wall concentration in presence of chemical reaction, American Journal of Computational and Applied Mathematics, 4(4) 141- 153,
DOI:0.5923/ j.ajcam.20140404.04.

Mohd Zuki Salleh,(2004), Mathematical models for the boundary layer flow due to a moving flat plate, Faculty of science, University Teknologi Malaysia.